International Journal of Thermophysics, Vol. 22, No. 6, November 2001 (© 2001)

Infinite Dilution Binary Diffusion Coefficients of Benzene in Carbon Dioxide by the Taylor Dispersion Technique at Temperatures from 308.15 to 328.15 K and Pressures from 6 to 30 MPa

T. Funazukuri,[1,2] C. Y. Kong,[3] and S. Kagei[3]

Received February 12, 2001

Infinite dilution binary diffusion coefficients, D_{12}, of benzene in carbon dioxide were measured by the Taylor dispersion technique at temperatures from 308.15 to 328.15 K and pressures from 6 to 30 MPa. The diffusion coefficients were obtained by the method of fitting in the time domain from the response curves measured with a UV–vis multidetector by scanning from 220 to 280 nm at increments of 1 or 4 nm. The wavelength dependences on the binary diffusion coefficient and the uncertainty were examined. The detector linearity, in terms of the relationship between the absorbance intensity and the product of the peak area of the response curve and CO_2 velocity, was found to fail at some characteristic absorption wavelengths such as 243, 248, 253, and 259 nm, even when the maximum absorbance intensities of the response curves were less than 0.5 and the fits were good. Although the D_{12} values obtained from the response curves measured at 253 nm were almost consistent with some literature data, the D_{12} values measured at wavelengths showing the detector linearity to be satisfactory, i.e., at 239 nm, were higher than those at 253 nm. The present D_{12} data at 239 nm were well represented by the Schmidt number correlation, except for those showing the anomalous decrease in a plot of D_{12} vs density in the density range from 250 to 500 $kg \cdot m^{-3}$.

KEY WORDS: benzene; binary diffusion coefficient; carbon dioxide; supercritical; Taylor dispersion.

[1] Department of Applied Chemistry, Institute of Science and Engineering, Chuo University, 1-13-27 Kasuga, Bunkyo-ku, Tokyo 112-8551, Japan.

[2] To whom correspondence should be addressed. E-mail: funazo@apchem.chem.chuo-u.ac.jp

[3] Graduate School of Environment and Information Sciences, Yokohama National University, 79-7 Tokiwadai, Hodogaya-ku, Yokohama 240-8501, Japan.

0195-928X/01/1100-1643/0 © 2001 Plenum Publishing Corporation

1. INTRODUCTION

Binary diffusion coefficients, D_{12}, are one of the important physical properties for describing mass transfer rates under supercritical conditions, and many efforts to measure D_{12} values have been made. Measurements for benzene in carbon dioxide have been reported by many investigators [1–14]. However, the values are not consistent, and the reason has not been well clarified. Levelt Sengers et al. [11] measured and compared the D_{12} values with those reported in the literature, together with those for toluene, and pointed out that the detector linearity of optical detectors employed is important to obtain accurate D_{12} data, in particular, in the near-critical region.

In measurements for acetone in supercritical carbon dioxide [15, 16], the authors have examined the pressure dependences on detector linearity in terms of the relationship between the injected amount and the product of the peak area and CO_2 velocity, peak symmetry (the half peak-width ratio of the frontal to the latter value at 10% peak height, S_{10}), fitting error, ε, and wavelength dependence on the D_{12} value determined by fitting the calculated response curve to that measured in the time domain. It was found that the accuracy decreased with decreasing pressure and the response curve became more distorted as the pressure approached the critical pressure, even at 313.2 K (reduced temperature $T_r = 1.03$).

In this study, binary diffusion coefficients of benzene in CO_2 were measured by the Taylor dispersion method with a UV–vis multidetector. The wavelength dependences on the D_{12} value, detector linearity, S_{10}, and ε were examined by scanning from 220 to 280 nm at increments of 1 nm. Moreover, the present D_{12} values were compared with those reported in the literature, and the discrepancy of the D_{12} data is discussed.

2. THEORY

The theory was described by Taylor [17] and developed by Aris [18]. In this study, the D_{12} value was obtained by fitting, in the time domain, the response curve calculated with the assumed D_{12} value to that measured experimentally [15, 16]. The D_{12} value was obtained so as to minimize the fitting error, defined by Eq. (1), between the measured and the calculated response curves.

$$\varepsilon = \left(\frac{\int_{t_1}^{t_2} \{C_{\text{exp}}(L,t) - C_{\text{cal}}(L,t)\}^2 \, dt}{\int_{t_1}^{t_2} \{C_{\text{exp}}(L,t)\}^2 \, dt} \right)^{\frac{1}{2}} \tag{1}$$

where $C_{exp}(L, t)$ and $C_{cal}(L, t)$ are the tracer concentrations measured and calculated, respectively, L is the length of the diffusion column, and t_1 and t_2 are the times at 10% peak height of the response curve ($t_1 < t_2$).

3. EXPERIMENTAL APPARATUS AND PROCEDURES

The experimental apparatus and the procedures are almost-identical to those in previous studies [15, 16], except for solute injection volumes. Liquid benzene (mainly 0.2 μl) was loaded into the diffusion column through an HPLC injector (Rheodyne 7125 or 7520) with the sampling rotor or loop volumes of 0.2, 0.5, and 1 μl. The response curves were measured by scanning at increments of 1 or 4 nm from 220 to 280 nm, and the signals were recorded at a time interval of 1.6 s per scan in a personal computer. The optical cell volume is 4 μl, and the path length is 5 mm. Benzene was obtained from Aldrich with a purity of 99.99% and used without further purification. Carbon dioxide was employed with a purity higher than 99.995% (Analyzed; Showa Tansan, Japan) and an H_2O content less than 50 ppm.

4. RESULTS AND DISCUSSION

4.1. Effect of Wavelength

Figure 1 shows the typical response curves at wavelengths of 239 and 254 nm for a single injection of 0.2 μl liquid benzene at 313.15 K and

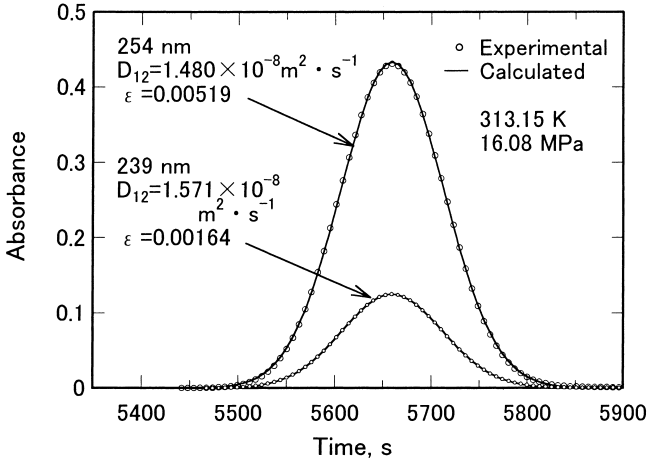

Fig. 1. Response curves calculated for the best fit and measured at 239 and 254 nm, 313.15 K, and 16.08 MPa.

16.08 MPa. A wavelength of 239 nm was employed in the present measurements as mentioned later. The absorbance intensity at 254 nm is about three times as high as that at 239 nm. The wavelength of about 254 nm has commonly been employed for measurements with a UV detector, whose wavelength is ascribed to the transition from π to π^* bonds of aromatic rings. It is found that the fits for the response curves at both wavelengths are quite good ($\varepsilon = 0.0016$ at 239 nm and 0.0052 at 254 nm). In previous studies [15, 16] we evaluated that the ε values less than 0.01 were a good fit, and those less than 0.02 were an acceptably good fit.

Figure 2 shows the wavelength dependences of (a) the absorbance intensity at the maximum peak height of the response curve, (b) the detector linearity in terms of the normalized absorbance intensity, *NAI*, equal to the maximum absorbance intensity divided by the value of (peak area) × (calculated CO_2 velocity; $u_{a,cal}$), (c) the root-mean-square fitting error, ε, and (d) the determined D_{12} value for the response curves, measured at 313.15 K and pressures of 11.09, 16.08, and 25.19 MPa, when measured at a resolution of 1 nm. It was found that five distinct characteristic peaks appeared at 238, 243, 248, 254, and 260 nm, and two small peaks at 233 and 268 nm. If the detector linearity is satisfactory, the *NAI* values should be constant. As shown in Fig. 2b, the detector linearity was found to fail at the four characteristic peaks, in particular, significantly at 247, 253, and 259 nm. The rms errors at the three characteristic absorbance wavelengths were higher than those at other wavelengths from 230 to 260 nm, while the values were still less than 0.01. However, the *NAI* values decreased, and correspondingly the D_{12} values decreased. Note that, strictly speaking, the wavelengths showing the absorbance peak maxima were slightly different from those showing the maximum rms errors, as well as the *NAI* value and D_{12} values, as shown in Figs. 2a to d.

If we choose the wavelengths of 237 to 240 and 243 to 246 nm, the D_{12} values are almost-constant and the rms errors are lower. When we choose the wavelengths showing the characteristic peaks around 247, 253, and 259 nm, the D_{12} values are inaccurate even if these show good fitting conditions, i.e., rms errors less than 0.01. Thus, the D_{12} values were obtained from the response curves at 239 nm in this study. Figure 3 shows D_{12}/T vs CO_2 viscosity for the present data measured at 239, 253, and 254 nm. This correlation has been found to be valid for various solutes in supercritical CO_2 [13, 15, 16, 19] and the mixture [20] as well as organic solvents [21]. It is found that the data at 239 nm can be represented by a straight line (solid), and those at 254 and 253 nm are also expressed with straight lines showing values lower by 6.7% (dashed–dotted) and 10% (dashed) than those at 239 nm, respectively.

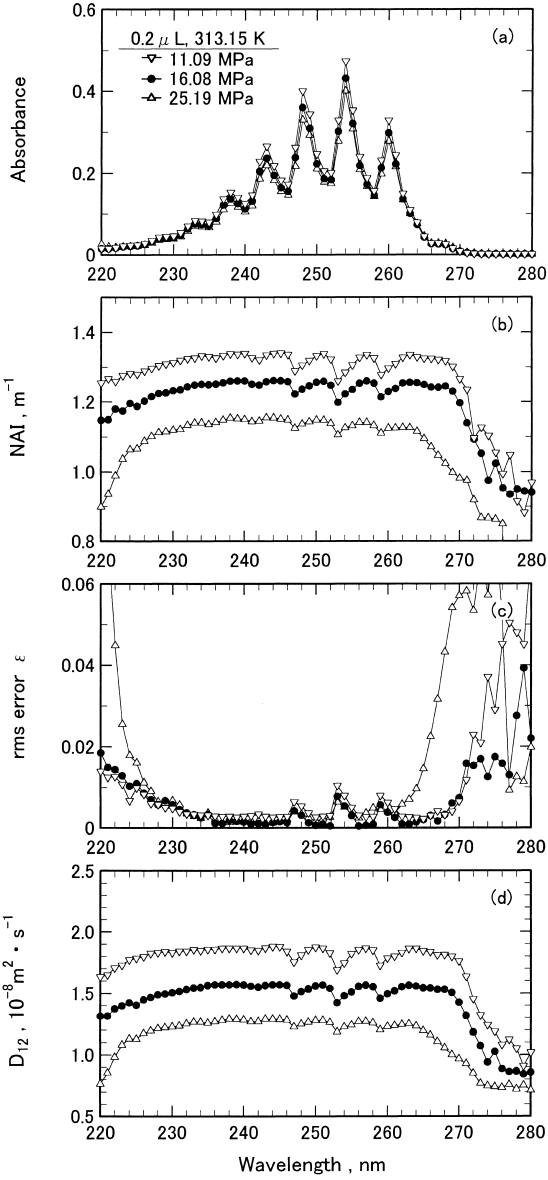

Fig. 2. Wavelength dependence on (a) absorbance intensity for the response curves at the maximum peak heights, (b) normalized absorbance intensity, *NAI*, (c) root mean square error, and (d) D_{12} values, measured at 313.15 K and pressures of 11.09, 16.08, and 25.19 MPa with 0.2 μl of liquid benzene injected.

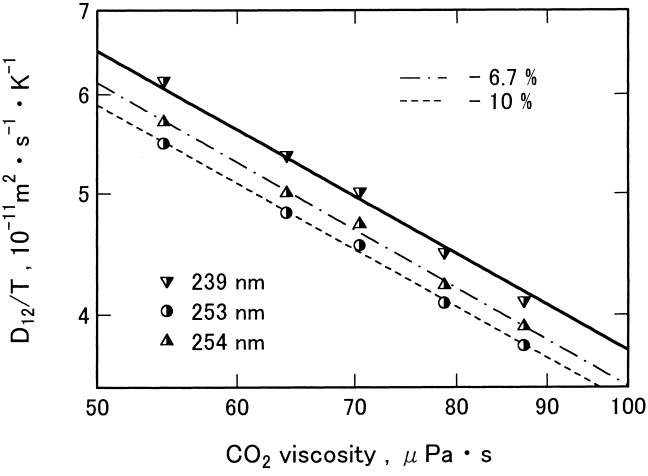

Fig. 3. D_{12}/T vs CO_2 viscosity for the present D_{12} data at 239, 253, and 254 nm and 313.15 K.

4.2. Effect of Secondary Flow

Figure 4 shows the effects of the secondary flow due to column coiling in plots of (a) D_{12}, (b) (peak area) $\times u_{a,cal}$, and (c) rms fitting error vs $DeSc^{1/2}$ at 313.15 K and 16.13 MPa, obtained at wavelengths of 239 and 255 nm, where De is the Dean number and Sc is the Schmidt number. According to Alizadeh et al. [22], the secondary flow effect was evaluated to be $< 1\%$ when the values of $DeSc^{1/2}$ were less than 8. The D_{12} values at the two wavelengths level off as the $DeSc^{1/2}$ values decrease, and the values of (peak area) $\times u_{a,cal}$ are also independent of the $DeSc^{1/2}$ value. In this study the measurements were made at $DeSc^{1/2}$ values less than 8, and the effect was negligible. Note that the relationship between D_{12} and $DeSc^{1/2}$ are similar at the two wavelengths, but the plateau values of D_{12} are different.

4.3. Effect of Amount Injected

Figure 5 shows the effects of the amount injected on (a) the absorbance spectra at the maximum peak height of the response curve, (b) the NAI value, (c) the rms fitting error, and (d) the determined D_{12} value, measured at 313.15 K and 16.08 MPa, for different injected amounts of benzene when 0.2, 0.5, and 1 μl liquid benzene were injected. The absorbance intensities for all cases were less than or almost equal to unity. The NAI values are constant, the fitting errors are low, and the D_{12} values are also independent of wavelength in the range from 230 to 240 nm. It should

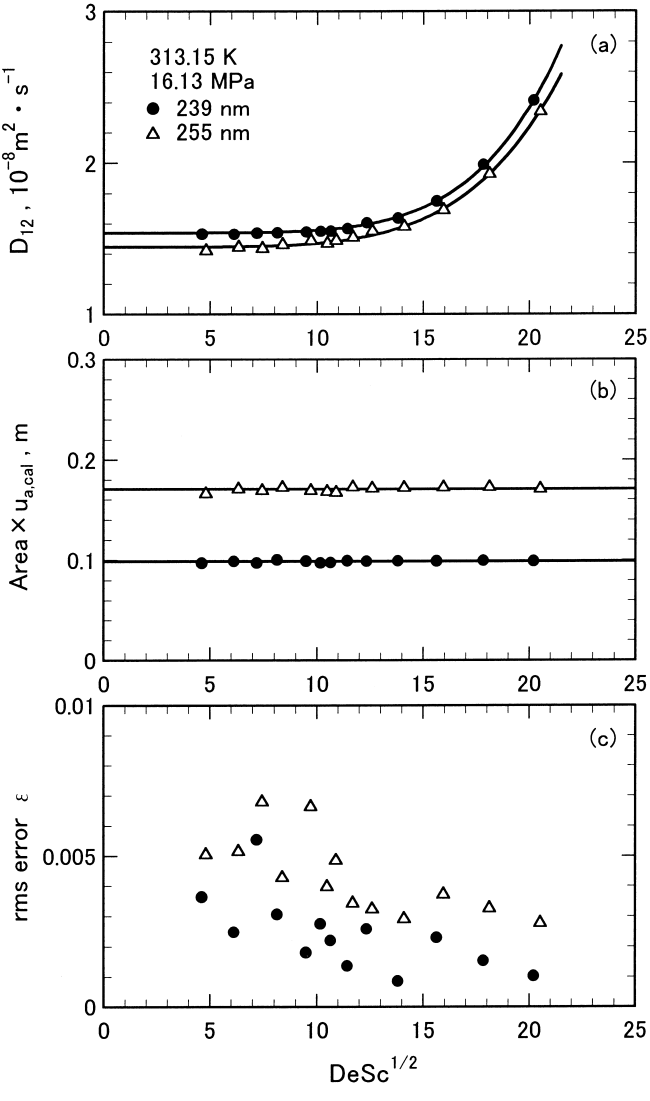

Fig. 4. Effect of the secondary flow on (a) D_{12} value, (b) area $\times u_{a,cal}$, and (c) rms error measured at 239 and 255 nm, 313.15 K, and 16.13 MPa with 0.5 μl of liquid benzene injected.

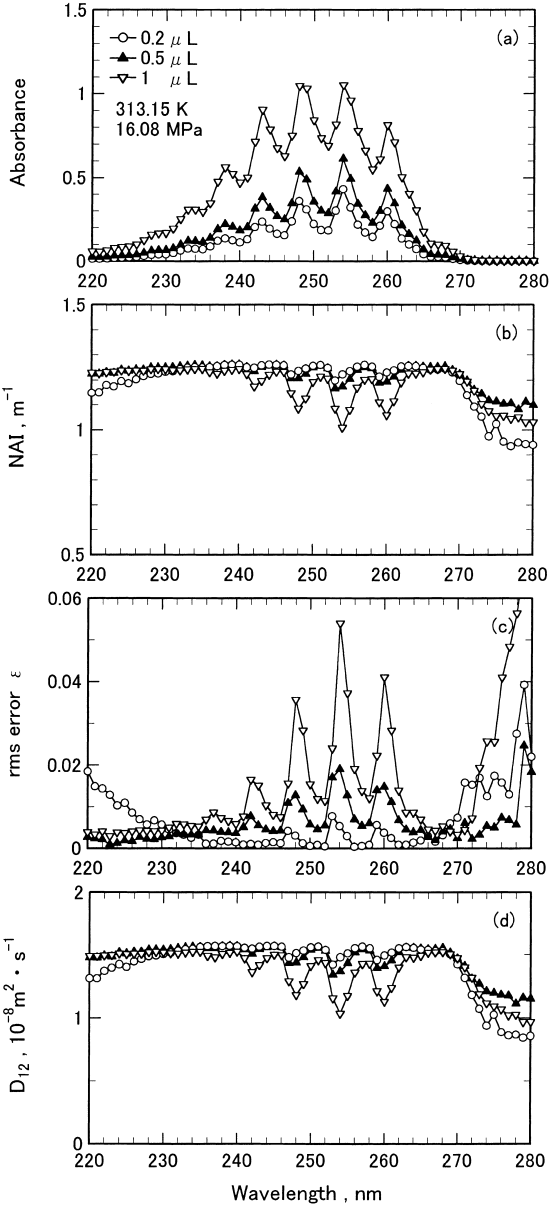

Fig. 5. Effect of amount of benzene injected on (a) absorbance intensities at the maximum peak heights of response curves, (b) *NAI* values, (c) rms error, and (d) D_{12} values, measured at 313.15 K and 16.08 MPa with 0.2, 0.5, and 1 μl benzene injected.

be noted that the detector linearity fails and the D_{12} values are also lower at 242, 248, 254, and 260 nm, although the absorbance intensities are lower than 0.7 for 0.2- and 0.5-μl injections. This observation suggests that the detector linearity should be carefully examined, in particular, when a large amount of tracer is injected, even though the wavelength showing a lower absorbance intensity is chosen.

4.4. D_{12} Values Determined

Figure 6 shows the effects of pressure on (a) the *NAI* value, (b) the S_{10} value, (c) the rms fitting error, and (d) the D_{12} values at the three temperatures of 308.15, 313.15, and 323.15 K, measured at 239 nm. Tables I to V also list the D_{12} values measured at 239 nm and all temperatures, together with fitting error. *NAI* value should simply increase with decreasing pressure, if the detector linearity holds, because D_{12} value increases with decreasing pressure. However, the *NAI* values at 308.15, 313.15, and 323.15 K show maximum values at about 8, 8, and 10 MPa, respectively. This suggests that the detector linearity fails and/or the *NAI* values are affected by the anomalous decease in D_{12} values in the near-critical regions. As the *NAI* values abruptly increase at 8 to 10 MPa, the values of S_{10} and rms error correspondingly increase, as shown in Figs. 6b and c. In the previous measurements of acetone [15], the products of (peak area) $\times u_{a,cal}$, S_{10} values, and rms errors were similarly observed to change remarkably with decreasing pressures below about 9 MPa, although the three values were almost independent of pressure at values higher than about 9 MPa. It is interesting that the values of *NAI*, S_{10}, and rms error tend to decrease at pressures lower than about 7 MPa.

4.5. Correlation

Figure 7 shows D_{12} values vs CO_2 density for all data listed in Tables I to V. At CO_2 densities higher than 500 $kg \cdot m^{-3}$ and lower than 210 $kg \cdot m^{-3}$, the D_{12} values can be represented by a solid line in Eq. (2), but the D_{12} values show a significant deviation from the smooth line at densities from 250 to 500 $kg \cdot m^{-3}$.

$$\ln\{10^8 D_{12}[m^2 \cdot s^{-1}]\} = \sum_{i=0}^{3} a_i (\ln\{\rho[kg \cdot m^{-3}]\})^i \tag{2}$$

where $a_0 = 53.0196$, $a_1 = -25.8336$, $a_2 = 4.41640$, and $a_3 = -0.258611$. As shown in Fig. 7, the deviated values correspond to the density region where

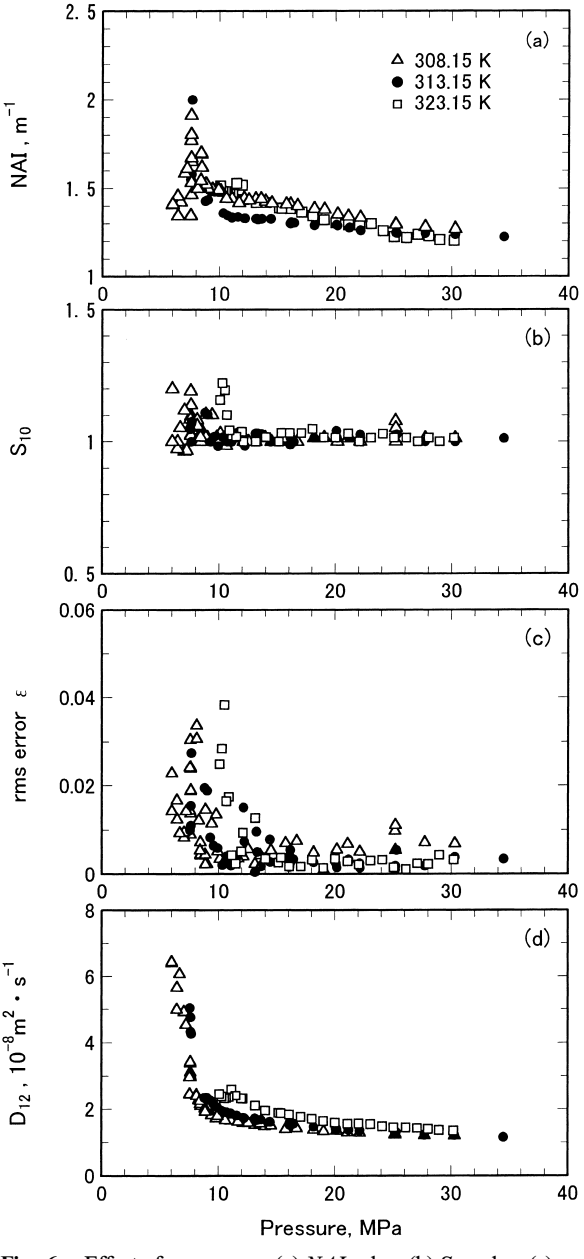

Fig. 6. Effect of pressure on (a) *NAI* value, (b) S_{10} value, (c) rms error, and (d) D_{12} value, measured at 239 nm and temperatures of 308.15, 313.15, and 323.15 K with 0.2 μl benzene injected.

Table I. Measured Binary Diffusion Coefficients of Benzene in Carbon Dioxide at 308.15 K

Pressure (MPa)	D_{12} (10^{-8} m$^2\cdot$s^{-1})	Fitting error ε	Pressure (MPa)	D_{12} (10^{-8} m$^2\cdot$s^{-1})	Fitting error ε	Pressure (MPa)	D_{12} (10^{-8} m$^2\cdot$s^{-1})	Fitting error ε
5.99	6.411	0.0228	8.12	2.401	0.0307	12.53	1.599	0.0057
5.99	6.442	0.0143	8.30	2.270	0.0122	13.11	1.529	0.0023
6.43	4.996	0.0167	8.41	2.253	0.0054	13.57	1.571	0.0043
6.44	5.663	0.0124	8.44	2.152	0.0072	13.94	1.487	0.0033
6.67	6.073	0.0093	8.44	2.153	0.0045	14.48	1.509	0.0055
7.03	4.918	0.0083	8.48	2.096	0.0043	15.75	1.403	0.0071
7.03	4.928	0.0094	8.85	2.018	0.0044	16.10	1.445	0.0044
7.21	4.542	0.0143	8.87	1.927	0.0022	16.70	1.427	0.0075
7.52	2.964	0.0144	8.88	1.922	0.0146	18.16	1.385	0.0050
7.53	2.453	0.0241	9.00	1.935	0.0023	19.03	1.337	0.0009
7.56	2.437	0.0305	9.41	1.814	0.0115	20.16	1.352	0.0056
7.58	3.110	0.0090	9.79	1.720	0.0135	21.09	1.302	0.0068
7.58	3.384	0.0188	9.92	1.792	0.0052	22.13	1.294	0.0051
7.59	3.408	0.0239	10.10	1.744	0.0035	25.14	1.244	0.0097
7.59	3.423	0.0242	10.59	1.663	0.0034	25.18	1.256	0.0054
7.59	3.028	0.0138	11.08	1.655	0.0031	25.18	1.236	0.0111
7.61	2.965	0.0190	11.66	1.623	0.0036	27.72	1.217	0.0072
8.11	2.424	0.0337	12.11	1.588	0.0041	30.29	1.204	0.0070

the detector linearity fails, and the S_{10} value and rms fitting error increase, as shown in Fig. 6. The deviation from the D_{12} values represented by the regression line in Eq. (2) probably results from the critical anomaly, and the failure of the detector linearity and the peak distortion are significant, as shown in Figs. 6a and b. More careful studies are required to justify the critical anomaly.

Table II. Measured Binary Diffusion Coefficients of Benzene in Carbon Dioxide at 313.15 K

Pressure (MPa)	D_{12} (10^{-8} m$^2\cdot$s^{-1})	Fitting error ε	Pressure (MPa)	D_{12} (10^{-8} m$^2\cdot$s^{-1})	Fitting error ε	Pressure MPa	D_{12} (10^{-8} m$^2\cdot$s^{-1})	Fitting error ε
7.55	5.047	0.0100	12.13	1.745	0.0151	18.16	1.468	0.0027
7.62	4.769	0.0110	12.20	1.727	0.0074	20.08	1.405	0.0025
7.62	4.331	0.0155	13.11	1.716	0.0005	20.16	1.402	0.0015
7.66	4.272	0.0275	13.22	1.690	0.0097	21.17	1.388	0.0034
8.80	2.344	0.0195	13.30	1.672	0.0051	21.18	1.381	0.0030
9.02	2.341	0.0189	13.62	1.680	0.0018	22.12	1.353	0.0025
9.29	2.270	0.0083	14.40	1.616	0.0079	22.15	1.371	0.0014
9.58	2.158	0.0065	14.42	1.612	0.0028	25.17	1.262	0.0010
9.92	2.060	0.0059	16.08	1.571	0.0016	25.19	1.285	0.0019
10.32	1.943	0.0021	16.11	1.531	0.0036	25.27	1.316	0.0055
10.70	1.914	0.0041	16.12	1.540	0.0031	27.71	1.233	0.0019
11.07	1.876	0.0019	16.13	1.531	0.0025	30.28	1.213	0.0039
11.09	1.858	0.0028	16.16	1.538	0.0056	34.48	1.162	0.0035
11.57	1.809	0.0040	16.43	1.568	0.0034			

Table III. Measured Binary Diffusion Coefficients of Benzene in Carbon Dioxide at 318.15 K

Pressure (MPa)	D_{12} (10^{-8} m$^2\cdot$s^{-1})	Fitting error ε	Pressure (MPa)	D_{12} (10^{-8} m$^2\cdot$s^{-1})	Fitting error ε	Pressure (MPa)	D_{12} (10^{-8} m$^2\cdot$s^{-1})	Fitting error ε
9.28	2.479	0.0248	16.05	1.664	0.0049	24.08	1.391	0.0039
9.60	2.389	0.0188	17.00	1.619	0.0017	25.00	1.376	0.0037
9.94	2.333	0.0086	17.98	1.571	0.0009	25.96	1.367	0.0046
10.18	2.465	0.0330	19.06	1.534	0.0031	27.07	1.369	0.0034
11.00	2.170	0.0068	20.06	1.498	0.0031	27.98	1.329	0.0047
11.96	1.991	0.0040	20.56	1.511	0.0045	29.03	1.317	0.0042
13.01	1.876	0.0101	21.07	1.466	0.0028	30.18	1.291	0.0055
14.03	1.806	0.0023	22.03	1.454	0.0030			
15.08	1.713	0.0032	23.03	1.429	0.0040			

Table IV. Measured Binary Diffusion Coefficients of Benzene in Carbon Dioxide at 323.15 K

Pressure (MPa)	D_{12} (10^{-8} m$^2\cdot$s^{-1})	Fitting error ε	Pressure (MPa)	D_{12} (10^{-8} m$^2\cdot$s^{-1})	Fitting error ε	Pressure (MPa)	D_{12} (10^{-8} m$^2\cdot$s^{-1})	Fitting error ε
10.09	2.456	0.0249	14.00	1.957	0.0035	23.05	1.548	0.0031
10.28	2.385	0.0285	15.13	1.887	0.0027	24.07	1.477	0.0033
10.49	2.330	0.0384	15.33	1.879	0.0038	25.03	1.449	0.0015
10.67	2.345	0.0165	16.07	1.835	0.0018	26.09	1.444	0.0011
10.88	2.367	0.0175	17.06	1.768	0.0017	27.06	1.425	0.0025
11.12	2.596	0.0043	18.03	1.709	0.0033	28.01	1.404	0.0023
11.47	2.408	0.0024	19.00	1.644	0.0014	28.96	1.367	0.0044
11.95	2.327	0.0052	20.00	1.595	0.0035	30.19	1.356	0.0033
12.08	2.318	0.0094	21.09	1.560	0.0029			
13.13	2.110	0.0127	22.05	1.566	0.0022			

Table V. Measured Binary Diffusion Coefficients of Benzene in Carbon Dioxide at 328.15 K

Pressure (MPa)	D_{12} (10^{-8} m$^2\cdot$s^{-1})	Fitting error ε	Pressure (MPa)	D_{12} (10^{-8} m$^2\cdot$s^{-1})	Fitting error ε	Pressure (MPa)	D_{12} (10^{-8} m$^2\cdot$s^{-1})	Fitting error ε
9.05	3.150	0.0459	13.43	2.231	0.0100	21.03	1.672	0.0026
9.74	2.854	0.0492	14.10	2.159	0.0029	21.99	1.638	0.0031
9.98	2.749	0.0147	15.08	2.040	0.0022	23.03	1.584	0.0042
9.99	2.740	0.0482	16.13	1.919	0.0016	23.96	1.598	0.0013
10.64	2.600	0.0373	16.90	1.894	0.0041	24.68	1.571	0.0025
11.24	2.466	0.0247	17.16	1.865	0.0010	25.75	1.528	0.0051
11.56	2.460	0.0174	17.99	1.840	0.0059	26.83	1.517	0.0033
12.07	2.464	0.0121	19.03	1.762	0.0017	29.23	1.454	0.0035
12.55	2.388	0.0111	19.78	1.715	0.0024			
13.14	2.325	0.0030	20.06	1.770	0.0020			

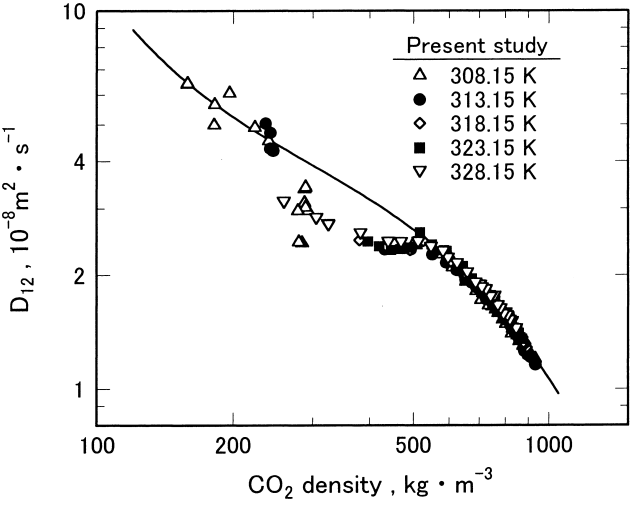

Fig. 7. D_{12} values vs CO_2 density at temperatures from 308.15 to 328.15 K for all data listed in Tables I to V.

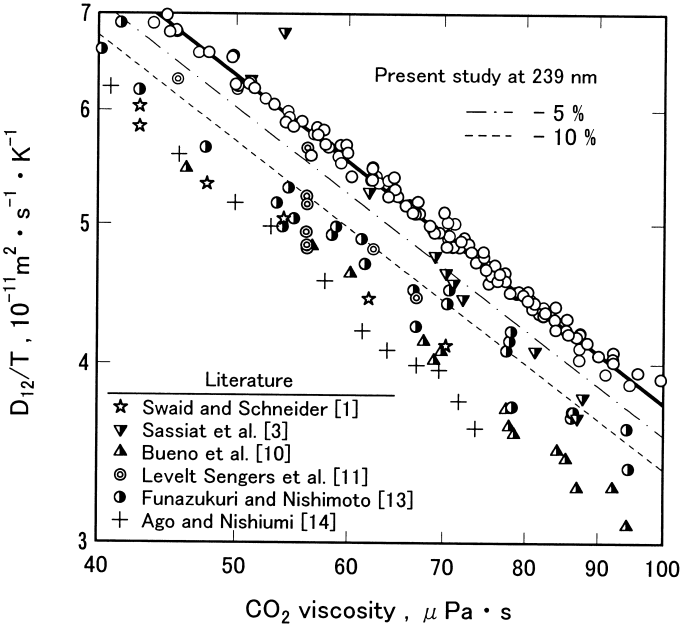

Fig. 8. D_{12}/T vs CO_2 viscosity for the present D_{12} data at 239 nm and literature data.

Figure 8 compares D_{12}/T vs CO_2 viscosity for the present D_{12} data at 239 nm with literature data [1, 3, 10, 11, 13, 14], all measured by the Taylor dispersion technique. The D_{12} data measured at 253 nm, located lower by about 10% than the present data at 239 nm (see Fig. 3), are almost consistent with the literature data [3, 11, 13]. This results partly in the difference between the present and the literature data. Unfortunately, the path lengths of optical cells and/or measuring wavelength were mostly not described in the literature, and one of the main reasons for the inconsistency of the D_{12} values can possibly be ascribed to the failure of detector linearity by measuring at characteristic wavelengths such as 253 nm. Note that Funazukuri and Nishimoto [13] measured at 255 to 270 nm with 0.2-μl injections, and Ago and Nishiumi [14] at 262 nm with 0.7 μl in the range of injected amounts from 0.7 to 13.1 μl.

Figure 9 shows a plot of the Schmidt number correlation [15, 23] together with deviations from the correlation and rms error for the present D_{12} data, where Sc^+ is the Schmidt number ratio of that at high pressure to that at atmospheric pressure at the same temperature, v is the molar volume of CO_2, and v_0 is the hard-sphere closest-packed volume, which is obtained from the correlation [8]. Note that the hard-sphere diameters for benzene determined by Dymond et al. [24] are 0.5119, 0.5114, 0.5110, 0.5106, and 0.5101 nm at 308.15, 313.15, 318.15, 323.15, and 328.15 K, respectively. The Schmidt number correlation has been confirmed to be valid for the D_{12} data on acetone [15, 16], ketones [16], phenol [19], α-tocopherol [19], β-carotene [19], naphthalene [25, 26], and dimethylnaphthalenes [26]. As depicted, at v_0/v values higher than 0.23 the D_{12} data are represented well by this correlation, but the D_{12} data deviate significantly in the v_0/v range from 0.1 to 0.23, which fully corresponds to those showing the deviation, as shown in Fig. 7. The plot seems to be asymptotic to the correlation at v_0/v values lower than 0.1, and the NAI values again lead to a constant value as shown in Fig. 6a.

Figure 10 shows plots of the Schmidt number correlation for literature data, together with deviations from the correlation. Most of the literature D_{12} data [1, 10, 11, 13, 14] are lower (the plots are higher) than those from the correlation over the entire range of v_0/v values.

5. CONCLUSIONS

Infinite dilution binary diffusion coefficients of benzene in sub- and supercritical carbon dioxide were measured by the Taylor dispersion technique. The effects of wavelength on the D_{12} values were examined. The detector linearity was found to fail for measurements at the characteristic wavelengths from 240 to 260 nm. The D_{12} data showing the failure of the

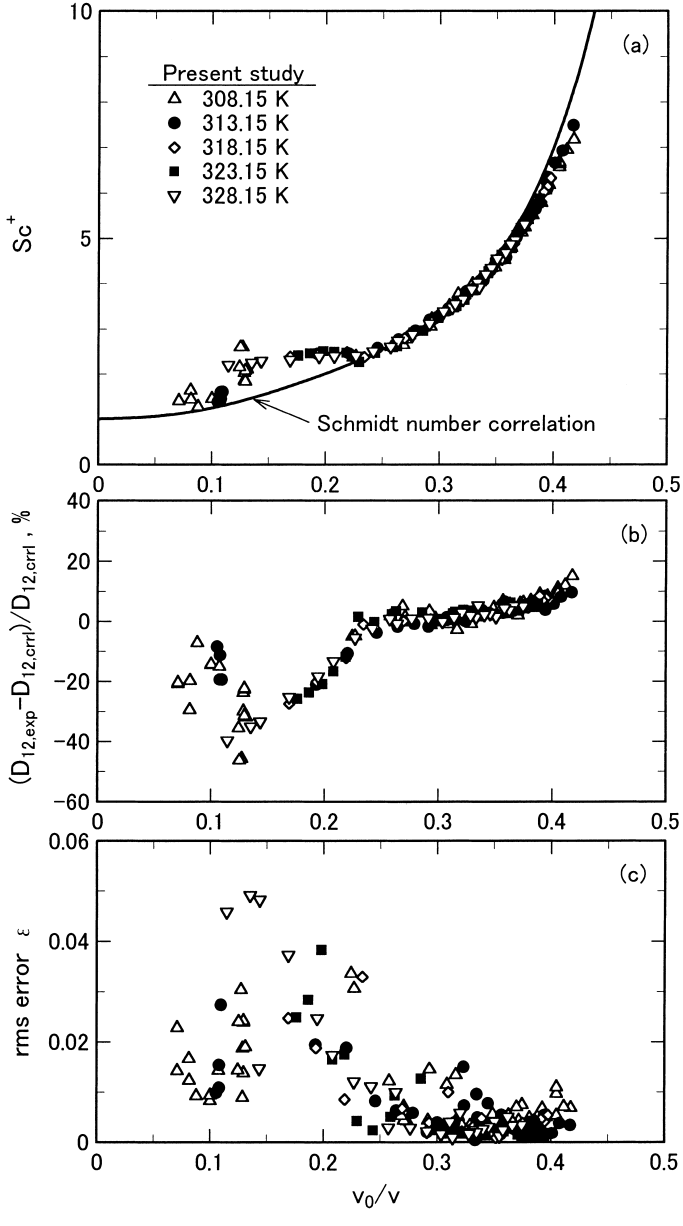

Fig. 9. Plot of (a) Schmidt number correlation, (b) deviation from the correlation, and (c) rms error, for all data listed in Tables I to V.

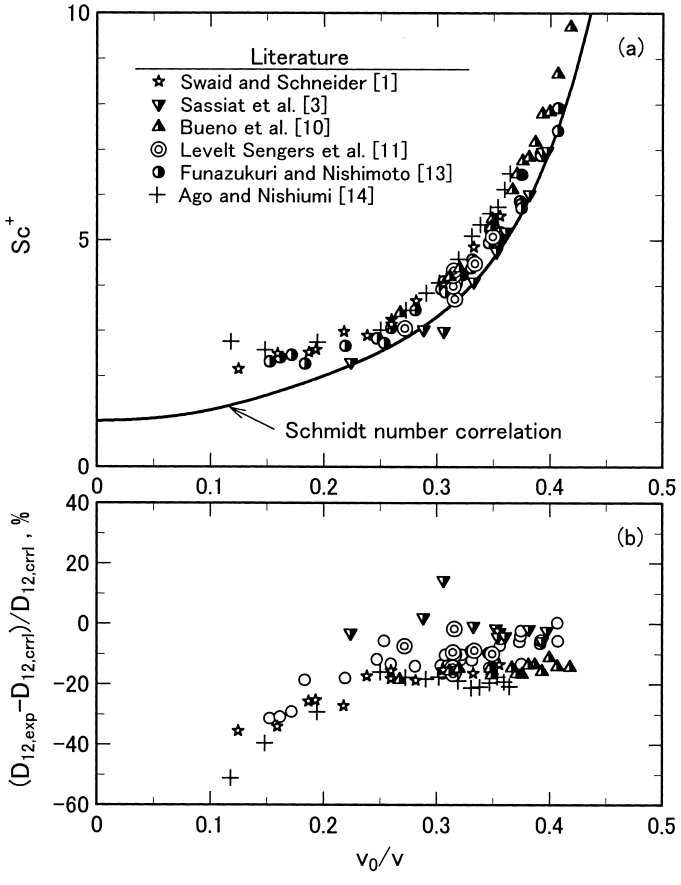

Fig. 10. Plot of (a) Schmidt number correlation for literature data and (b) deviation from the correlation.

detector linearity result in lower D_{12} values, while the lower values are nearly consistent with literature data. The D_{12} values at 239 nm were well represented by the Schmidt number correlation, except for $v_0/v = 0.1$ to 0.23, where the D_{12} values indicate an anomalous decrease, and the response curves were significantly distorted. In this region the detector linearity also failed.

ACKNOWLEDGMENTS

The authors are grateful to the Takahashi Industrial and Economic Research Foundation for financial support. The authors also thank the

Promotion and Mutual Aid Corporation for Private Schools of Japan for a project research grant (Development of Molecular Functional Materials) and the Ministry of Education, Culture, Sports, Science and Technology through a Grant-in-Aid for Scientific Research.

NOMENCLATURE

C	Tracer concentration
De	Dean number
D_{12}	Binary diffusion coefficient
L	Column length
NAI	Normalized absorbance intensity
Sc	Schmidt number
Sc^+	Ratio of Schmidt number at high pressure to that at atmospheric pressure
S_{10}	Ratio of the latter half to the front width at 10% peak height
T	Temperature
t	Time
t_1, t_2	Time at 10% peak height of response curve ($t_1 < t_2$)
u_a	Average carbon dioxide velocity
v	Molar volume of carbon dioxide
v_0	Hard-sphere closest-packed volume of carbon dioxide
ε	Error defined by Eq. (1)

Subscripts

exp	Experiment
cal	Calculation
crrl	Correlation

REFERENCES

1. I. Swaid and G. M. Schneider, *Ber. Bunsenges. Phys. Chem.* **83**:969 (1979).
2. R. Feist and G. M. Schneider, *Sep. Sci. Technol.* **17**:261 (1982).
3. P. R. Sassiat, P. Mourier, M. H. Caude, and R. H. Rosset, *Anal. Chem.* **59**:1164 (1987).
4. T. Funazukuri, S. Hachisu, and N. Wakao, *Anal. Chem.* **61**:118 (1989).
5. C. Erkey, H. Gadalla, and A. Akgerman, *J. Supercrit. Fluids* **3**:180 (1990).
6. T. Funazukuri, S. Hachisu, and N. Wakao, *Ind. Eng. Chem. Res.* **30**:1323 (1991).
7. S. V. Olesik and J. L. Woodruff, *Anal. Chem.* **63**:670 (1991).
8. T. Funazukuri, Y. Ishiwata, and N. Wakao, *AIChE J.* **38**:1761 (1992).
9. S. Umezawa and A. Nagashima, *J. Supercrit. Fluids* **5**:242 (1992).
10. J. L. Bueno, J. J. Suárez, J. Dizy, and I. Medina, *J. Chem. Eng. Data* **38**:344 (1993).
11. J. M. H. Levelt Sengers, U. K. Deiters, U. Klask, P. Swidersky, and G. M. Schneider, *Int. J. Thermophys.* **14**:893 (1993).

12. J. J. Suárez, J. L. Bueno, and I. Medina, *Chem. Eng. Sci.* **48**:2419 (1993).
13. T. Funazukuri and N. Nishimoto, *Fluid Phase Equil.* **125**:235 (1996).
14. K. Ago and H. Nishiumi, *J. Chem. Eng. Jpn* **32**:563 (1999).
15. T. Funazukuri, C. Y. Kong, and S. Kagei, *Int. J. Thermophys.* **21**:651 (2000).
16. T. Funazukuri, C. Y. Kong, and S. Kagei, *Int. J. Thermophys.* **21**:1279 (2000).
17. G. Taylor, *Proc. Roy. Soc. London A* **219**:186 (1953).
18. R. Aris, *Proc. Roy. Soc. London A* **235**:67 (1956).
19. T. Funazukuri, C. Y. Kong, and S. Kagei, *Ind. Eng. Chem. Res.* **39**:4462 (2000).
20. T. Funazukuri and Y. Ishiwata, *Fluid Phase Equil.* **164**:117 (1999).
21. T. Funazukuri, N. Nishimoto, and N. Wakao, *J. Chem. Eng. Data* **39**:911 (1994).
22. A. Alizadeh, C. A. Nieto de Castro, and W. A. Wakeham, *Int. J. Thermophys.* **1**:243 (1980).
23. T. Funazukuri and N. Wakao, Preprint of the AIChE fall meeting, New Orleans (1993).
24. J. H. Dymond, *J. Phys. Chem.* **85**:3291 (1981).
25. H. Higashi, Y. Iwai, Y. Takahashi, H. Uchida, and Y. Arai, *Fluid Phase Equil.* **144**:269 (1998).
26. H. Higashi, Y. Iwai, Y. Nakamura, S. Yamamoto, and Y. Arai, *Fluid Phase Equil.* **166**:101 (1999).